One-neutron stripping from ^{9}Be to ^{169}Tm, ^{181}Ta, and ^{187}Re at near-barrier energies

Y. D. Fang,[1,*] P. R. S. Gomes,[2,†] J. Lubian,[2] J. L. Ferreira,[2] D. R. Mendes Junior,[2] X. H. Zhou,[1] M. L. Liu,[1] N. T. Zhang,[1] Y. H. Zhang,[1] G. S. Li,[1] J. G. Wang,[1] S. Guo,[1] Y. H. Qiang,[1] B. S. Gao,[1,3] Y. Zheng,[1] X. G. Lei,[1] and Z. G. Wang[1,3]

[1]*Institute of Modern Physics, Chinese Academy of Sciences, Lanzhou 730000, People's Republic of China*

[2]*Instituto de Física, Universidade Federal Fluminense, Avenida Litoranea s/n, Gragoatá, Niterói, Rio de Janeiro, 24210-340, Brazil*

[3]*Graduate University of Chinese Academy of Sciences, Beijing, 000049, People's Republic of China*

(Received 28 January 2016; published 17 March 2016)

We report the measurement of one-neutron stripping of ^{9}Be to the ^{169}Tm, ^{181}Ta, and ^{187}Re nuclei, in the range from subbarrier to above-barrier energies. The activation technique was used, with the detection of off-line γ rays. The results show that the transfer cross sections for the three systems investigated are very similar and are much larger than the corresponding fusion cross sections at subbarrier energies, whereas fusion predominates at energies above the barrier. Data are in good agreement with our coupled reaction channel calculations. We also investigate the ratio, as a function of energy, between experimental transfer and fusion cross sections. The role of transfer couplings on the fusion excitation functions is also discussed.

DOI: 10.1103/PhysRevC.93.034615

I. INTRODUCTION

Reactions and scattering of weakly bound nuclei have been widely investigated in the last years, especially fusion, breakup, and elastic scattering [1–4]. Several reaction processes may occur after the breakup of one of the colliding nuclei (we will consider as the projectile): sequential complete fusion (SCF) if all fragments fuse with the target, incomplete fusion (ICF) if only part of the projectile fuses, and noncapture breakup when neither fragments fuse with the target. However, some direct processes may also occur, without the breakup of the weakly bound nucleus, such as direct complete fusion (DCF) or direct transfer of nucleons or clusters of nucleons.

Systematic results [3,5–10] have shown that the coupling effects of the breakup channel on the complete fusion (CF) suppress its cross section at energies above the Coulomb barrier and produce some enhancements at subbarrier energies.

Direct transfer reactions are the less-investigated processes involving weakly bound nuclei. One usually finds in the literature that, when transfer and incomplete fusion lead to the same nucleus, the measured cross section is attributed only to the latter, and the direct transfer is neglected. Thus, transfer process may lead to some complications in experimental and theoretical studies of fusion. One example is the ICF cross section in collisions of weakly bound projectiles like ^{6}Li. In this case, the direct transfer of a ^{2}H or a ^{4}He cluster produces the same final states as the ICF of the corresponding fragment, after ^{6}Li breakup. From the experimental point of view, these processes cannot be distinguished and usually, when one reports the measurement of ICF, the measurement was actually of the sum of both processes.

On the other hand, from the theoretical point of view, transfer and ICF are very different processes. The former takes place in a single step whereas the latter is a two-step process (breakup and then partial fusion). At subbarrier energies, ICF occurs after a tunneling of part of the projectile whereas in direct transfer no tunneling is required. Since direct transfer and breakup processes do not need to tunnel through the barrier, their excitation functions do not drop as fast as the fusion excitation function at subbarrier energies, and those processes may have larger cross sections than fusion at energies below the Coulomb barrier. This fact can also be indirectly observed in some precise elastic scattering experiments with weakly bound nuclei, where it is clear that the Coulomb barrier is not the threshold for reactions, since the imaginary part of the optical potential vanishes at energies around 15% to 20% lower than the Coulomb-barrier energy [11].

Transfer reactions are particularly important in collisions of neutron-halo nuclei, such as ^{6}He, when the neutron-stripping cross sections are very large, mainly at subbarrier energies [12–21]. For experiments with neutron halo projectiles it was found that the one- and/or two-neutron transfer channels are the dominant processes below the Coulomb barrier and are still important at energies above the barrier.

Similar conclusions were reached for collisions of stable weakly bound projectiles, especially at subbarrier energies. Shrivastava *et al.* [22] measured one-neutron stripping and one-neutron pickup in the ^{6}Li + ^{198}Pt collision. They have shown that the direct reaction cross section is much larger than the fusion cross section at energies below the barrier. They also investigated the ^{7}Li + ^{198}Pt system [23] and found that the one- and two-neutron stripping and the one-neutron pickup reactions have important cross sections. Palshetkar *et al.* [24] investigated ^{6,7}Li + ^{197}Au collisions and found sizable transfer cross sections for reactions induced by ^{6}Li (one-neutron stripping and one-neutron pickup) and by ^{7}Li (one- and two-neutron stripping). Di Pietro *et al.* [25] investigated the ^{6,7}Li + ^{64}Zn collision. They concluded that CF is the main process at above-barrier energies whereas transfer is the dominant processes below the Coulomb barrier [26].

However, for ^{9}Be-induced reactions, there are very few reported works on transfer reactions above or below the barrier,

*Present address: Research Center for Nuclear Physics, Osaka University, Ibaraki, Osaka 567-0047, Japan; fangyd@impcas.ac.cn

†paulogom@if.uff.br

all of them for one-neutron-stripping measurements [27–29]. Our group has reported the measurement of one-neutron stripping of ^{9}Be to ^{186}W at only one energy above the barrier [30]. To contribute to the investigation of transfer reactions induced by the ^{9}Be nucleus, we performed experiments with the ^{169}Tm, ^{181}Ta, and ^{187}Re targets at energies near the Coulomb barrier (above and below), using the off-line γ-ray spectroscopy method. Direct one-neutron-stripping transfer could be identified and their cross sections measured. The transfer Q values for the tree systems are similar and very positive: +4.93, +4.40, and +4.21 MeV for ^{169}Tm, ^{181}Ta, and ^{187}Re, respectively.

From the theoretical side, since the breakup feeds states in the continuum, and transfer may also feed states in the continuum, the most suitable theoretical approach to describe breakup and its influence on fusion might be the continuum discretized coupled channel (CDCC) method. However, the CDCC method is still far from giving a satisfactory description of collisions of weakly bound nuclei. In most cases it does not lead to individual CF and ICF cross sections nor can it take into account bound and continuum states of the projectile simultaneously with nucleon transfer or inelastic channels in the target. When the projectile breaks into three particles, such as ^{6}He into $^{4}\mathrm{He} + n + n$ or ^{9}Be into $n + \alpha + \alpha$, the four-body CDCC calculations are even more difficult to do. Transfer reactions are usually theoretically investigated through coupled reaction channel (CRC) or distorted wave Born approximation (DWBA) calculations, as we do in the present work.

In the present paper, in Sec. II we describe the experimental setup. In Sec. III we show the experimental one-neutron transfer cross sections obtained for the three systems. In Sec. IV we compare our data with CRC calculations. In Sec. V we discuss the relations between the fusion and transfer excitation functions and the transfer coupling effect on the fusion cross section. Finally, we summarize our work and present some conclusions.

II. EXPERIMENT PROCEDURE

The neutron-stripping cross sections for the $^{9}\mathrm{Be} + {}^{169}$Tm, ^{181}Ta, and ^{187}Re systems were obtained through a standard stacked-foil irradiation followed by off-line measurement of the γ ray of the activation products by using high-resolution high-purity Ge (HPGe) setups. A full description of the experimental technique and setup has been presented in Ref. [31]; here only a brief description and additional information relevant to the neutron transfer cross sections are given. The experiments were performed at the sector focusing cyclotron in the Heavy Ion Research Facility Lanzhou (HIRFL), China. Stacks of ^{169}Tm, ^{181}Ta, and ^{187}Re targets were irradiated with a collimated ^{9}Be beam with an initial energy of 50.4 MeV. For each type of target, two stacks were prepared with each stack having eight targets. To trap the recoiling residues produced during irradiation as well as to reduce the energy of the beam on the subsequent target of the stack, each target was backed with Al foil of thickness around 1 mg/cm^2. The typical average thickness of ^{169}Tm targets was around 600 μg/cm^2, while the thickness of ^{181}Ta and ^{187}Re targets were in the range of 430 to 590 μg/cm^2 and 310 to 370 μg/cm^2, respectively. To obtain the irradiation at beam energies of 32–40 MeV, an Al degrader foil with a thickness of 11.1 mg/cm^2 was placed in front of the stack. The energy losses in the target layer, in the Al backing, and in the Al degrader foil were determined by using ATIMA calculations within the LISE++ program [32,33]. The beam current was determined from the charge collected in a Faraday cup behind the target stack by using a precision current-integrator device. The current-integrator counts were recorded in the acquisition, stepping every second, to obtain the beam current as a function of time during the irradiation.

After the end of the irradiation, the activity of the targets was measured by using HPGe detectors. For the residue nucleus ^{188}Re in the $^{9}\mathrm{Be} + {}^{187}$Re system, the same HPGe setup was used as in our previous paper [31]. As for the residue ^{170}Tm, since it has a long half-life ($T_{1/2} = 128$ d, $I^{\pi} = 1^{-}$) and only a weak (2.48%), low-energy 84.3 keV γ line is emitted in its decay, the activity measurement was carried out about one month after the irradiations by using a commercial ORTEC Compton Suppression Counting Systems (to this end, the average laboratory background count rate is reduced to about 3 s^{-1}). During the cooling period of more than one month, the activities of other reaction products formed in the $^{9}\mathrm{Be} + {}^{169}$Tm system decreased by a factor of more than 1000; therefore, the background is significantly suppressed in the low-energy region. The same ORTEC Compton Suppression Counting Systems was used to measure the activity of ^{182}Ta in the $^{9}\mathrm{Be} + {}^{181}$Ta system, but a longer cooling time of two months was chosen. Typical measured γ-ray spectra are shown in Fig. 1, where the γ lines of interest are clearly identified. To confirm that the γ lines observed are coming from the residues of interest, the half-life for each residue was followed. As an example, in Fig. 2 we show the activity curve for the ^{188}Re peak (155 keV line); the half-life extracted from our measurements is in agreement with data in the literature [34].

III. EXPERIMENTAL RESULTS

The experimentally measured one-neutron stripping cross sections in $^{9}\mathrm{Be} + {}^{169}$Tm, ^{181}Ta, and ^{187}Re systems are given in Table I. As the experimental method used was the off-line γ-ray spectroscopy, the transfer cross sections measured are the total cross sections to the ground state and to all excited states.

Figure 3 shows the one-neutron-stripping excitation functions for the three systems investigated. The Coulomb-barrier energies are indicated in the figure with arrows. One can observe that, at energies below the Coulomb barrier, the excitation functions do not drop as fast as one usually observes for fusion excitation functions. This may be explained by the peripheral character of direct transfer reactions, which do not require tunneling through the barrier. One observes a saturation of the transfer cross sections around 150 mb for the three systems, at high energies. One can also observe some small decrease for the ^{181}Ta target at the two highest energies, corresponding to $1.33V_B$ and $1.36V_B$ and for the ^{169}Tm target at the highest energy, corresponding to $1.36V_B$. This might be explained by the competition with other reaction mechanisms

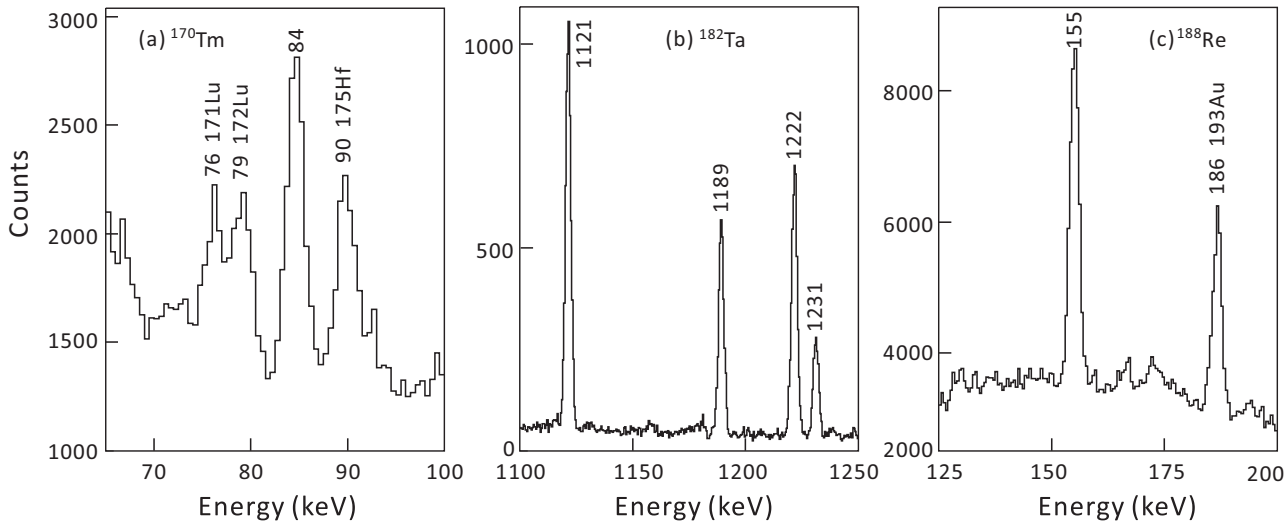

FIG. 1. Off-line γ-ray spectra (a) for ^{9}Be + ^{169}Tm system showing the 84 keV γ line emitted in the decay of ^{170}Tm, measured 37 days after the end of activation with a collection time of 2 days, (b) for ^{9}Be + ^{181}Ta system showing the 1121, 1189, 1222, and 1231 keV γ lines emitted in the decay of ^{182}Ta, measured 60 days after the end of activation with a collection time of 2 days, and (c) for ^{9}Be + ^{187}Re system showing the 155 keV γ line emitted in the decay of ^{188}Re, measured 8 hours after the end of activation with a collection time of 1 hour.

at this energy region. For the ^{187}Re target one cannot see the decrease, but for this system the highest energy measured corresponds to $1.31V_B$, for which there is also no decrease of the transfer cross section for the other two systems.

The one-neutron transfer excitation functions are very similar for the three systems. This behavior is somehow expected, since they have similar transfer Q values and we were able to measure only the total transfer cross section, rather than transfer to specific states.

The small differences between the three excitation functions may be partially explained by the fact that the sizes and heights of the Coulomb barrier are slightly different. A solution to compare different systems would be the use of some reduction procedure. However, recently it has been shown [35,36] that, although there is a suitable method to reduce fusion excitation functions [37], there is not an available method that can properly reduce direct reaction and total reaction cross sections. Thus, we did not use any reduction method in the present work.

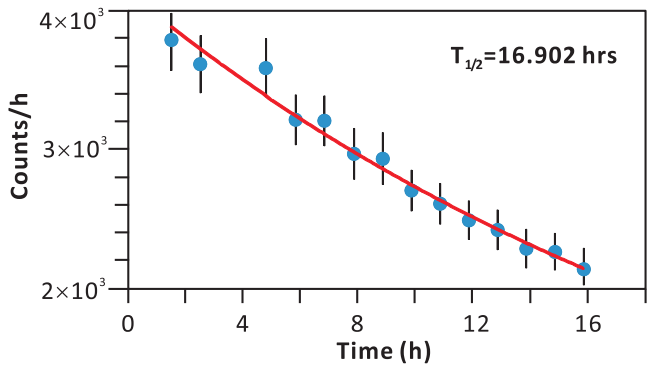

FIG. 2. Activity curve for the ^{188}Re nucleus formed in ^{9}Be + ^{187}Re reaction by using the 155 keV line.

IV. COMPARISON OF TRANSFER CROSS-SECTION DATA WITH COUPLED REACTION CHANNEL CALCULATIONS

In this section we show the comparison of the experimental data shown in the previous section with the results of calculations. We performed coupled reaction channel (CRC) calculations for the $1n$ stripping reaction of ^{9}Be and ^{169}Tm. We performed the calculations for only one system because they are very computer time consuming and we believe that the verification whether our transfer data could be explained by the calculations would be similar for the three systems. There was no particular reason for the choice of the system with the ^{169}Tm target.

To perform this calculations there are various important ingredients such as the optical potential, spectroscopic amplitudes, and form-factors needed for coupled channel calculations. For the real and imaginary parts of the optical potential, the double-folding Saõ Paulo potential was used [38,39]. At near barrier energies this potential is a usual double-folding potential with the advantage that has a comprehensive systematic for the matter densities. For this reason this is a parameter-free potential.

Because the breakup channel was not considered in our calculations, polarization potentials that account for this important reaction channel have to be added to the potential of the entrance partition (to the optical potential of the elastic channel). This was achieved by the inclusion of the strength coefficients $N_R = N_I = 0.6$. The strength coefficients for the real parts have been shown to account for the repulsive character of the real part of the breakup polarization potential [40,41]. The strength for the imaginary part was introduced by Pereira *et al.* [42] to account for the loss of flux due to dissipative processes. In the case of breakup channels, it accounts for the imaginary part of the polarization potential [40]. A Woods–Saxon imaginary potential with parameters $W = 50.0$ MeV, $r_w = 1.06$ fm, and $a_w = 0.2$ fm for the depth,

TABLE I. Measured cross sections for the production of one-neutron-stripping residue in the ^{9}Be + ^{169}Tm, ^{181}Ta, and ^{187}Re systems.

^{9}Be + ^{169}Tm		^{9}Be + ^{181}Ta		^{9}Be + ^{187}Re	
E_{lab} (MeV)	^{170}Tm (mb)	E_{lab} (MeV)	^{182}Ta (mb)	E_{lab} (MeV)	^{188}Re (mb)
48.0	148.5 ± 12.3	50.3	124.9 ± 11.5	49.1	157.7 ± 11.3
46.9	155.9 ± 15.9	49.2	131.7 ± 8.0	48.1	155.6 ± 10.4
45.7	153.2 ± 13.0	48.1	145.3 ± 10.2	47.2	161.4 ± 10.9
44.5	156.0 ± 12.5	47.0	147.6 ± 9.4	46.2	151.3 ± 9.2
43.2	152.3 ± 9.6	45.9	150.2 ± 19.1	45.0	147.7 ± 9.9
42.0	153.9 ± 10.1	44.7	142.4 ± 11.7	44.0	152.3 ± 8.8
40.2	137.1 ± 9.5	43.5	140.8 ± 9.1	42.7	157.9 ± 9.2
38.9	143.8 ± 8.8	42.3	147.4 ± 10.0	40.3	153.1 ± 9.1
37.7	120.0 ± 7.1	40.3	141.4 ± 8.9	39.2	149.6 ± 9.5
36.3	116.8 ± 6.6	39.0	130.1 ± 8.5	38.0	122.5 ± 7.6
35.0	90.8 ± 5.8	37.8	125.2 ± 7.5	36.8	95.3 ± 6.1
33.5	64.2 ± 4.5	36.5	98.1 ± 5.4	35.5	75.6 ± 4.5
32.1	42.3 ± 3.0	35.3	71.5 ± 5.3	34.2	51.6 ± 3.2
		33.9	70.1 ± 19.2	32.9	34.3 ± 2.1
		32.5	38.0 ± 10.0		

reduced radius, and diffuseness, respectively, was considered in the entrance partition (^{9}Be + ^{169}Tm) to account for the loss of flux to fusion (but not included in the solution of the system of coupled equations). This potential is internal to the barrier and guaranties that the flux that passed through or over the Coulomb barrier is accounted for fusion.

For the final partition (^{8}Be + ^{170}Tm), the Saõ Paulo potential was used for both real and imaginary parts with strength coefficients $N_R = 1.0$ and $N_I = 0.78$, respectively. This approach has been proved to be suitable for describing the elastic scattering cross sections for several systems [43] over a wide energy interval.

The spectroscopic amplitudes for projectile and target overlaps were set equal to 1.0. The reason for that is that, to calculate the overlaps between nuclei with charge larger than 28 (Ni isotopes), usually it is required to use a very large model space, which is quite difficult to handle even with the computer facilities that are available nowadays. This is the case of the present target overlaps. In the case of the projectile overlaps, although the model space is much smaller, we decided to set the spectroscopic amplitudes also equal to 1.0 and to interpret our results as an approximate.

The projectile overlaps considered in the calculations are shown in Fig. 4. One should notice that two-step processes were also included in the coupling scheme; that is, the transfer from the $5/2^-$ resonance state at 2.429 MeV to the 2^+ resonant state of ^{8}Be at 3.030 MeV. For the excitation of this $L = 2$ resonant state, we considered that this is a bound state, because it lives for a time larger than the reaction time. The rotational model has been used to describe this coupling, including the reorientations terms. The deformation parameter was taken from Ref. [44] as equal to $\beta_2 = 0.92$.

The target overlaps considered in the CRC calculations are shown in Fig. 5. The second-order overlaps from the excited state $3/2^+$ at 0.008 MeV of ^{169}Tm are identified as dot-dot-dashed lines in this figure to facilitate their identification, since several other overlaps have been considered in the calculations. For the excitation of the $L = 2\ 3/2^+$ state, the rotational model was considered. The deformation parameter $\beta_2 = 0.326$ [45] of the neighbor ^{170}Yb was taken, similar to what has been done in our previous study of the fusion cross section [31].

For both projectile and target, Woods–Saxon form factors were used with reduced radii $r_0 = 1.2$ fm and diffuseness

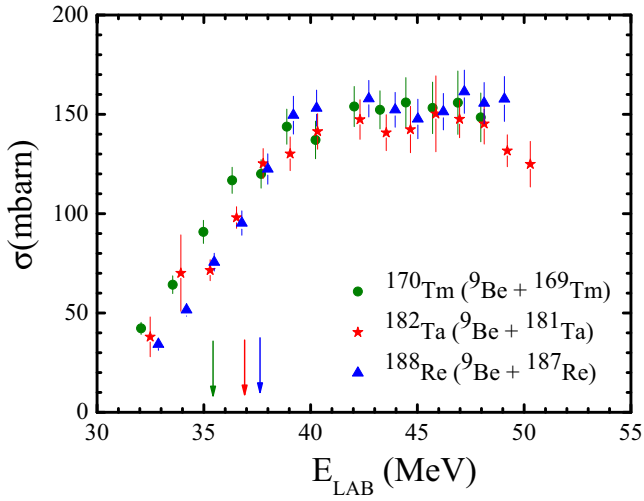

FIG. 3. Measured one-neutron-stripping excitation functions for ^{9}Be + ^{169}Tm, ^{181}Ta, and ^{187}Re systems.

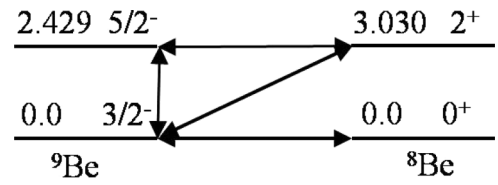

FIG. 4. Scheme of coupling for the projectile overlaps considered in the CRC calculations.

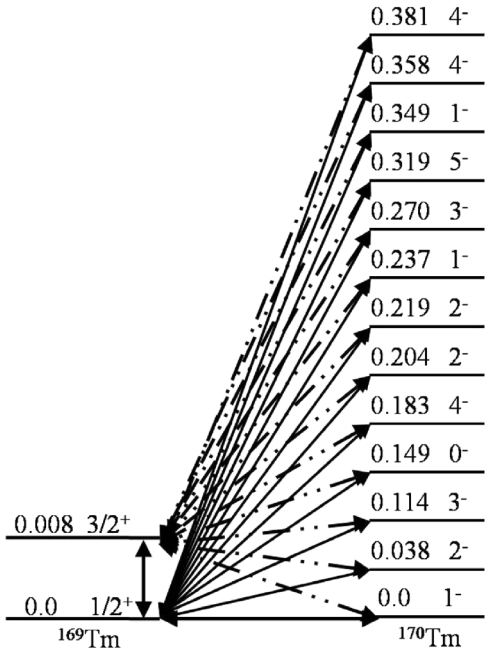

FIG. 5. Scheme of coupling for the target overlaps considered in the CRC calculations.

$a_0 = 0.65$ fm to generate the single-particle wave functions of the neutrons. The depth of the potential was varied to fit the experimental neutron binding energies. The spin-orbital interaction was also included with standard depth of 7 MeV.

For the CRC calculation, the prior exact finite-range approximation was used, including the full complex remnant terms and nonorthogonality corrections. All calculations were performed by using FRESCO code [46]. In Fig. 6 the results

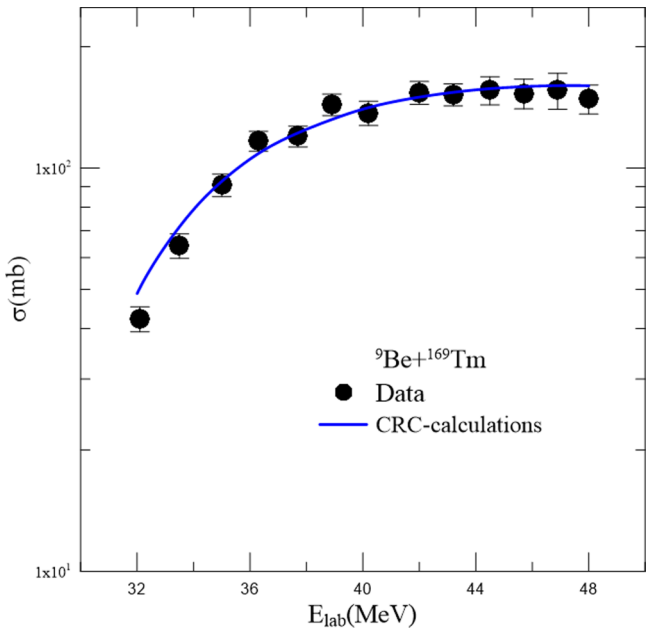

FIG. 6. Comparison of experimental transfer (one neutron stripping) cross sections measured in the present work for the ^{9}Be + ^{169}Tm reaction (symbols) and the results of our CRC calculations (curve).

of CRC calculations are compared with the experimental data of the one-neutron transfer reaction ^{169}Tm(^{9}Be , ^{8}Be) ^{170}Tm. One can see a rather good agreement between the theory and the experiment in the whole energy interval studied in the present work.

V. DISCUSSION OF TRANSFER AND FUSION CROSS SECTIONS

It would be interesting to compare the transfer excitation functions measured in the present work for the three systems with the fusion cross sections for the same systems. The fusion data are already available [31,47]. Figure 7 shows the transfer and complete fusion excitation functions for the three systems, separately. The behavior for the three systems is similar. One can observe that, at subbarrier energies, the transfer cross sections are much larger than the fusion cross sections. This is expected since direct transfer is a peripheral process and does not require the tunneling of the barrier to occur. On the other hand, for energies above the barrier, the fusion process clearly predominates over direct transfer, which saturates at energies not too much above the Coulomb barrier.

One can notice that, with the logarithmic scale of Fig. 7, one cannot observe the small decrease in the transfer cross sections at the highest energies, as was possible with the linear scale of Fig. 3.

The comparison between transfer and fusion cross sections as a function of the energy can be more clearly investigated by the plot of the ratio between these cross sections as a function

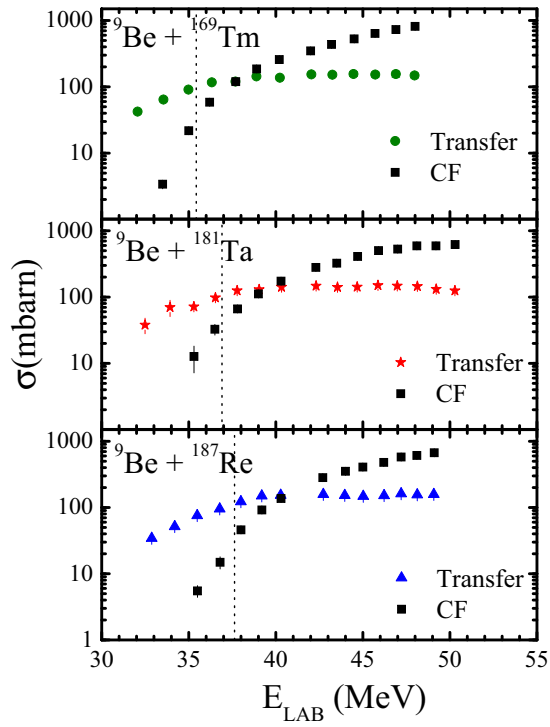

FIG. 7. Transfer (one-neutron stripping) cross sections measured in the present work for the three systems and the complete fusion excitation functions for the same systems, reported in Refs. [31,47]. The energies of the Coulomb barriers are represented by the dashed vertical line.

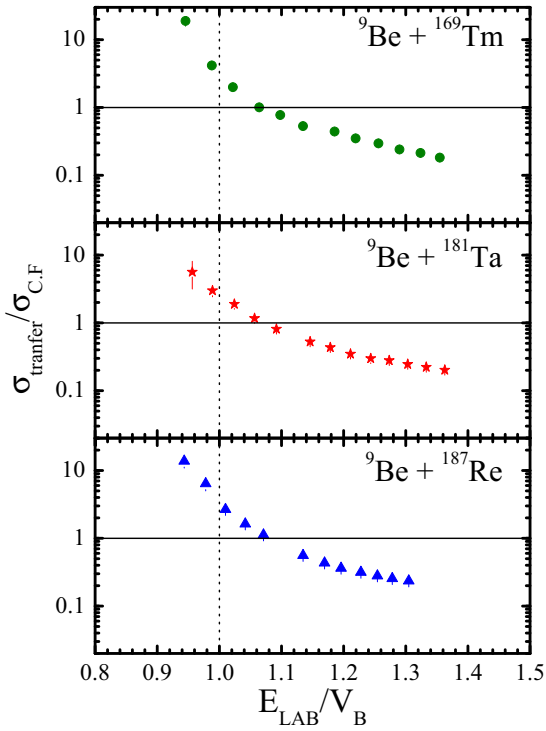

FIG. 8. Ratios between transfer (one-neutron stripping) cross sections measured in the present work for the three systems and the complete fusion excitation functions for the same systems, reported in Refs. [31,47], as a function of the energy relative to the Coulomb barrier.

of the quantity $E_{\rm lab}/V_B$, where V_B is the Coulomb barrier. The results are shown in Fig. 8. One can observe that, for the three systems, this ratio is around 20% at the highest energy, which is around 35% above the Coulomb-barrier energy. At the barrier energy, the transfer cross section is around twice the fusion cross section, and at the lowest energies, of the order of 0.87 to $0.90V_B$, the transfer cross section is around ten times the fusion cross section, or even more than that. We interpret these results, as already mentioned, by the fact that, for the fusion process at subbarrier energies to occur, tunneling through the barrier is required, whereas the direct one-neutron-stripping transfer process does not require tunneling.

Finally, we make comments on the role of the coupling of the one-neutron transfer channel on the complete fusion excitation function. Although there are signatures that transfer channels with large Q values or large cross sections may couple with fusion and contribute to its enhancement at subbarrier energies, the relationship between transfer cross section and the effect of transfer channels on fusion is not straightforward, because they take place at different distances or correspond mostly to different angular momenta. Only transfer reactions which occur at distances not so far from the position of the Coulomb barrier are the natural candidates to behave as a doorway to fusion and enhance the subbarrier fusion cross section [48]. For the three systems investigated in the present work, it has been previously shown [31,47] that coupled channel calculations including only inelastic excitations were able to explain the full complete fusion-excitation functions. This means that the one-neutron transfer channels, although they have large cross sections at subbarrier energies, do not significantly influence the coupling scheme to the fusion process. The reason, as explained by Gomes *et al.* [48] from a semiclassical approach [see Fig. 4(d) in that paper], is that the transfer form factor for this transfer channel might not be too steep; that is, its value at the Coulomb-barrier region is not too high. For transfer processes of two or more particles, the transfer form factors are usually steeper and have more influence on the fusion process if they have a reasonable cross section. In summary, for the transfer cross section, the integral of transfer form factors at any distances outside the barrier is the important parameter, whereas for the influence of transfer on fusion (or effect of transfer couplings on fusion), what really matters is the integral of the form factor at a small region close to the Coulomb-barrier position. For the systems investigated in the present work, the transfer couplings do not play an important role in subbarrier fusion.

VI. SUMMARY AND CONCLUSIONS

We measured the excitation functions of one-neutron stripping of ^{9}Be to three different nuclei, in the range from subbarrier to above-barrier energies, by using the activation technique and detection of off-line γ rays. The results show that the total transfer cross sections for the three systems investigated are similar and they are much larger than the corresponding fusion cross sections at subbarrier energies, whereas fusion predominates at energies above the barrier. At energies around 10% below the Coulomb barrier, the ratio between transfer and fusion cross section is around ten, decreasing to two at the barrier energy and becoming around 0.2 at energies of the order of 30% above the barrier. This is interpreted as owing to the fact that, contrary to the fusion process, direct transfer processes do not need to tunnel through the Coulomb barrier.

CRC calculations for one of the investigated systems are in good agreement with the data. It is important to mention that, in the calculations, we assumed the spectroscopic amplitudes of projectile and target as equal to one and we also included in the coupling scheme the ^{9}Be $5/2^{-}$ resonance state at 2.429 MeV to the 2^{+} resonant state of ^{8}Be at 3.030 MeV, which has a significant role in the results.

Although the one-neutron-stripping transfer cross sections are significant at subbarrier energies, the effect of this channel on the subbarrier fusion excitation function is negligible, since it has already reported that the couplings of inelastic excitations are enough to explain the behavior of the fusion excitation functions for the three systems under investigation. We interpret that the reason is that most of the transfer reactions might occur at distances much larger than the Coulomb-barrier position.

ACKNOWLEDGMENTS

The authors wish to thank the staffs of HIRFL for the operation of the cyclotron and friendly collaboration during the experiment. C. J. Lin, H. M. Jia, and V. V. Parkar are gratefully

acknowledged. P. R. S. Gomes also thanks the CUSTIPEN (China-US Theory Institute for Physics with Exotic Nuclei), since his attendance at the workshop in Beijing helped him to go to Lanzhou to finish the present work. This work was supported by the National Natural Sciences Foundation of China (Grants No. U1232124, No. 10905075, and No. 11305221), the Major State Basic Research Development Program of China (Grant No. 2013CB834403), the ADS project No. 302 (Y103010ADS) and Youth Innovation Promotion Association of the Chinese Academy of Sciences. P. R. S. Gomes and J. Lubian acknowledge the partial support from CNPq, FAPERJ, and from Pronex.

[1] L. F. Canto, P. R. S. Gomes, R. Donangelo, and M. S. Hussein, Phys. Rep. **424**, 1 (2006).
[2] B. B. Back, H. Esbensen, C. L. Jiang, and K. E. Rehm, Rev. Mod. Phys. **86**, 317 (2014).
[3] L. F. Canto, P. R. S. Gomes, R. Donangelo, J. Lubian, and M. S. Hussein, Phys. Rep. **596**, 1 (2015).
[4] P. R. S. Gomes, J. Lubian, L. F. Canto, D. R. Otomar, D. R. Mendes Junior, P. N. de Faria, R. Linares, L. Sigaud, J. Rangel, J. L. Ferreira *et al.*, Few-Body Syst. **57**, 165 (2016).
[5] L. F. Canto, P. R. S. Gomes, J. Lubian, L. C. Chamon, and E. Crema, Nucl. Phys. A **821**, 51 (2009).
[6] H. Kumawat, V. Jha, V. V. Parkar, B. Roy, S. K. Pandit, R. Palit, P. K. Rath, C. F. Palshetkar, S. K. Sharma, S. Thakur *et al.*, Phys. Rev. C **86**, 024607 (2012).
[7] M. K. Pradhan, A. Mukherjee, P. Basu, A. Goswami, R. Kshetri, S. Roy, P. R. Chowdhury, M. S. Sarkar, R. Palit, V. V. Parkar *et al.*, Phys. Rev. C **83**, 064606 (2011).
[8] B. Wang, W. J. Zhao, P. R. S. Gomes, E. G. Zhao, and S. G. Zhou, Phys. Rev. C **90**, 034612 (2014).
[9] Bing Wang, Wei-Juan Zhao, Alexis Diaz-Torres, En-Guang Zhao, and Shan-Gui Zhou, Phys. Rev. C **93**, 014615 (2016).
[10] P. R. S. Gomes, L. F. Canto, J. Lubian, and M. S. Hussein, Phys. Lett. B **695**, 320 (2011).
[11] J. M. Figueira, J. O. F. Niello, A. Arazi, O. A. Capurro, P. Carnelli, L. Fimiani, G. V. Martí, D. M. Heimann, A. E. Negri, A. J. Pacheco *et al.*, Phys. Rev. C **81**, 024613 (2010).
[12] R. Raabe, J. L. Sida, J. L. Chavet, N. Alamanos, C. Angulo, J. M. Casandjian, S. Courtin, A. Drouart, C. Durand, P. Figuera *et al.*, Nature (London) **431**, 823 (2004).
[13] A. Di Pietro, P. Figuera, F. Amorini, C. Angulo, G. Cardella, S. Cherubini, T. Davinson, D. Leanza, J. Lu, H. Mahmud *et al.*, Phys. Rev. C **69**, 044613 (2004).
[14] A. Lemasson, A. Navin, N. Keeley, M. Rejmund, S. Bhattacharyya, A. Shrivastava, D. Bazin, D. Beaumel, Y. Blumenfeld, A. Chatterjee *et al.*, Phys. Rev. C **82**, 044617 (2010).
[15] A. Lemasson, A. Shrivastava, A. Navin, M. Rejmund, N. Keeley, V. Zelevinsky, S. Bhattacharyya, A. Chatterjee, G. de France, B. Jacquot *et al.*, Phys. Rev. Lett. **103**, 232701 (2009).
[16] Y. E. Penionzhkevich, R. Astabatyan, N. Demekhina, G. Gulbekian, R. Kalpakchieva, A. A. Kulko, S. Lukyanov, E. R. Markaryan, V. Maslov, and Y. E. R. Muzychka *et al.*, Eur. Phys. J. A **31**, 185 (2007).
[17] E. F. Aguilera, J. J. Kolata, F. M. Nunes, F. D. Becchetti, P. A. De Young, M. Goupell, V. Guimarães, B. Hughey, M. Y. Lee, D. Lizcano *et al.*, Phys. Rev. Lett. **84**, 5058 (2000).
[18] E. F. Aguilera, J. J. Kolata, F. D. Becchetti, P. A. DeYoung, J. D. Hinnefeld, A. Horváth, L. O. Lamm, H. Y. Lee, D. Lizcano, E. Martinez-Quiroz *et al.*, Phys. Rev. C **63**, 061603(R) (2001).
[19] L. Acosta, A. M. Sánchez-Benítez, M. E. Gómez, I. Martel, F. Pérez-Bernal, F. Pizarro, J. Rodríguez-Quintero, K. Rusek, M. A. G. Alvarez, M. V. Andrés *et al.*, Phys. Rev. C **84**, 044604 (2011).
[20] A. Navin, V. Tripathi, Y. Blumenfeld, V. Nanal, C. Simenel, J. M. Casandjian, G. de France, R. Raabe, D. Bazin, A. Chatterjee *et al.*, Phys. Rev. C **70**, 044601 (2004).
[21] A. Chatterjee, A. Navin, A. Shrivastava, S. Bhattacharyya, M. Rejmund, N. Keeley, V. Nanal, J. Nyberg, R. G. Pillay, K. Ramachandran *et al.*, Phys. Rev. Lett. **101**, 032701 (2008).
[22] A. Shrivastava, A. Navin, A. Lemasson, K. Ramachandran, V. Nanal, M. Rejmund, K. Hagino, T. Ishikawa, S. Bhattacharyya, A. Chatterjee *et al.*, Phys. Rev. Lett. **103**, 232702 (2009).
[23] A. Shrivastava, A. Navin, A. Diaz-Torres, V. Nanal, K. Ramachandran, M. Rejmund, S. Bhattacharyya, A. Chatterjee, S. Kailas, A. Lemasson *et al.*, Phys. Lett. B **718**, 931 (2013).
[24] C. F. Palshetkar, S. Thakur, V. Nanal, A. Shrivastava, N. Dokania, V. Singh, V. V. Parkar, P. C. Rout, R. Palit, R. G. Pillay *et al.*, Phys. Rev. C **89**, 024607 (2014).
[25] A. Di Pietro, P. Figuera, E. Strano, M. Fischella, O. Gorynov, M. Lattuada, C. Maiolino, C. Marchetta, M. Milin, A. Musumarra *et al.*, Phys. Rev. C **87**, 064614 (2013).
[26] S. P. Hu, G. L. Zhang, J. C. Yang, H. Q. Zhang, P. R. S. Gomes, J. Lubian, J. L. Ferreira, X. G. Wu, J. Zhong, C. Y. He, Y. Zheng, C. B. Li, G. S. Li, W. W. Qu, F. Wang, L. Zheng, L. Yu, Q. M. Chen, P. W. Luo, H. W. Li, Y. H. Wu, W. K. Zhou, B. J. Zhu, and H. B. Sun, Phys. Rev. C **93**, 014621 (2016).
[27] D. J. Hinde, M. Dasgupta, B. R. Fulton, C. R. Morton, R. J. Wooliscroft, A. C. Berriman, and K. Hagino, Phys. Rev. Lett. **89**, 272701 (2002).
[28] R. J. Woolliscroft, N. M. Clarke, B. R. Fulton, R. L. Cowin, M. Dasgupta, D. J. Hinde, C. R. Morton, and A. C. Berriman, Phys. Rev. C **68**, 014611 (2003).
[29] C. Signorini, Eur. Phys. J. A **13**, 129 (2002).
[30] Y. D. Fang, P. R. S. Gomes, J. Lubian, X. H. Zhou, Y. H. Zhang, J. L. Han, M. L. Liu, Y. Zheng, S. Guo, J. G. Wang *et al.*, Phys. Rev. C **87**, 024604 (2013).
[31] Y. D. Fang, P. R. S. Gomes, J. Lubian, M. L. Liu, X. H. Zhou, D. R. Mendes Junior, N. T. Zhang, Y. H. Zhang, G. S. Li, J. G. Wang *et al.*, Phys. Rev. C **91**, 014608 (2015).
[32] G. Scheidenberger and H. Geissel, Nucl. Instrum. Methods Phys. Res., Sect. B **135**, 25 (1985).
[33] D. Bazin, O. Tarasov, M. Lewitowicz, and O. Sorlin, Nucl. Instrum. Methods Phys. Res., Sect. A **482**, 307 (2002).
[34] http://www.nndc.bnl.gov/ensdf/.
[35] L. F. Canto, D. R. Mendes Junior, P. R. S. Gomes, and J. Lubian, Phys. Rev. C **92**, 014626 (2015).
[36] P. R. S. Gomes, D. R. Mendes Junior, L. F. Canto, J. Lubian, and P. N. de Faria, Few-Body Syst. **57**, 205 (2016).
[37] L. F. Canto, P. R. S. Gomes, J. Lubian, L. C. Chamon, and E. Crema, J. Phys. G **36**, 015109 (2009).

[38] L. C. Chamon, D. Pereira, M. S. Hussein, M. A. Candido Ribeiro, D. Galetti, Phys. Rev. Lett. **79**, 5218 (1997).
[39] L. C. Chamon, B. V. Carlson, L. R. Gasques, D. Pereira, C. De Conti, M. A. G. Alvarez, M. S. Hussein, M. A. Cândido Ribeiro, E. S. Rossi, Jr., and C. P. Silva, Phys. Rev. C **66**, 014610 (2002).
[40] D. P. Sousa, D. Pereira, J. Lubian, L. C. Chamon, J. R. B. Oliveira, E. S. Rossi, Jr, C. P. Silva, P. N. de Faria, V. Guimarães, R. Lichtenthäler *et al.*, Nucl. Phys. A **836**, 1 (2010).
[41] Y. Sakuragi, M. Yahiro, and M. Kamimura, Prog. Theor. Phys. **70**, 1047 (1983).
[42] D. Pereira, L. J., J. R. B. Oliveira, D. P. de Sousa, and L. C. Chamon, Phys. Lett. B **670**, 330 (2009).
[43] L. R. Gasques, L. C. Chamon, P. R. S. Gomes, and J. Lubian, Nucl. Phys. A **764**, 135 (2006).
[44] M. Dasgupta, P. R. S. Gomes, D. J. Hinde, S. B. Moraes, R. M. Anjos, A. C. Berriman, R. D. Butt, N. Carlin, J. Lubian, C. R. Morton *et al.*, Phys. Rev. C **70**, 024606 (2004).
[45] S. Raman, C. Nestor, Jr., and P. Tikkanen, At. Data Nucl. Data Tables **78**, 1 (2001).
[46] I. J. Thompson, Comput. Phys. Rep. **7**, 167 (1988).
[47] N. T. Zhang, Y. D. Fang, P. R. S. Gomes, J. Lubian, M. L. Liu, X. H. Zhou, G. S. Li, J. G. Wang, S. Guo, Y. H. Qiang *et al.*, Phys. Rev. C **90**, 024621 (2014).
[48] P. R. S. Gomes, A. M. M. Maciel, R. M. Anjos, S. B. Moraes, R. Liguori Neto, R. Cabezas, C. Muri, G. M. Santos, and J. F. Liang, J. Phys. G **23**, 1315 (1997).